

## **CHAPTER 5**

### **POWER SYSTEMS UNDER DEREGULATION**

In the previous chapter modeling of a two area AGC under conventional scenario was carried out. The fuzzy logic controllers optimized using GA for a two area AGC has been shown to be better in terms of performance indices as compared to conventional controllers.

In this chapter multi-area AGC design and modeling is presented under restructured scenario. The emphasis has been laid out in designing the intelligent controllers under the restructured scenario. Various clues from previous papers [37]-[44] are taken to implement intelligent techniques for efficient use of the controllers. A common practical model [45] of a two area AGC under restructured scenario is considered for simulation and analysis. Sensitivity analysis is carried out to check the robustness of the designed controllers. Additionally a novel approach is used to test the intelligent controllers under dynamically changing system parameters. The system is also tested for random step load pattern injected at random intervals of time.

#### **5.1 INTRODUCTION TO RESTRUCTURED AGC**

The development and the procedure of the power system have to be reformulated in a restructured power system keeping the vital ideas the same [46]-[49]. Many countries have switched over to the restructuring of the power system around the world. At present the power business is run by vertically integrated utilities (VIUs) which own generation, transmission and distribution systems. These VIUs supply power to the consumers at regulated tariffs. The general configuration of VIU is shown in Fig. 5.1

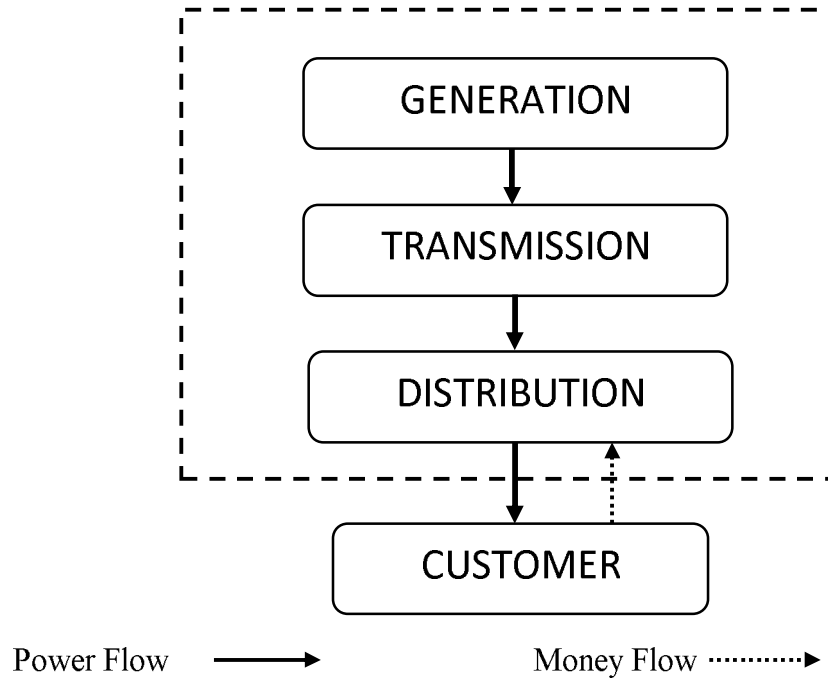


Figure 5.1 Structure of Vertically Integrated Utility (VIU)

In the present situation, the first step towards deregulation will be to split the generation of power from the transmission and distribution. The generating companies termed as GENCOs are free to compete and sell power which they produce. The retail customers will now purchase power from local distribution companies which are designated as DISCOs. The entities that circulate the power between GENCOs and DISCOs are termed as TRANSCOs. The utility structure after deregulation is shown in Fig. 5.2

With the advent of the different characteristics of GENCOs, TRANSCOs, DISCOs, the ancillary services of a VIU will have a distinct contribution and therefore there is a need for its modeling [50], [51]. Since Automatic Generation Control (AGC) is one of the ancillary services, it is required to be modeled. Now under this situation, a DISCO can contract alone with a GENCO for power under the regulation of ISO.

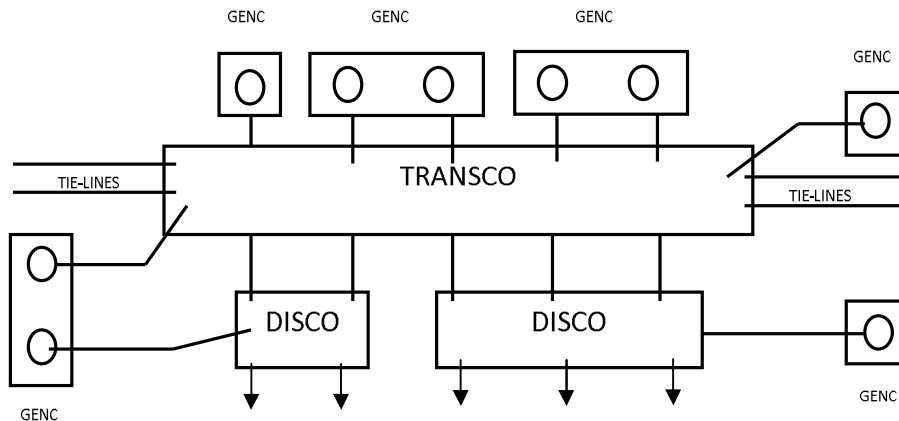


Figure 5.2 Utility Structures after Deregulation

## 5.2 CONVENTIONAL VS RESTRUCTURED SYSTEM

In section 5.1 VIU and deregulated utility structures have been discussed. Since there are a number of GENCOs and DISCOs in the restructured scenario, a DISCO has the liberty to choose any GENCO for contract of power. A DISCO may contract power with a GENCO in another control area. Such types of deals are called bilateral transactions. All such transactions have to be implemented under the purview of an unbiased entity called an independent system operator (ISO). The ISO has a task of controlling various ancillary services. One of the important services is the AGC.

## 5.3 CONCEPT OF DISCO PARTICIPATION

After Deregulation, GENCOs vend power to different DISCOs with a competition in prices [52]. Thus, there is a freedom for the DISCOs to choose GENCOs for buying power. Also a DISCO may not necessarily have contracts with the GENCOs in their own area; they may choose a GENCO from other areas as well. As a result numerous combinations are valid for DISCO and GENCO

transactions. To understand the contracts, DISCO participation matrix (DPM) is described which has rows and columns equal to the number of GENCOs and the number of DISCOs respectively in the system. A two area interconnected system comprising two GENCOS and two DISCOS in each area are considered.

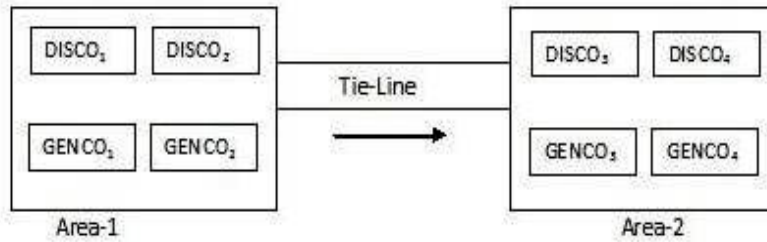


Figure 5.3 Configuration of a two area system under Restructured scenario

The equivalent DPM for the system shown in Fig. 5.3 is illustrated in the Table 5.1

Table 5.1 DPM corresponding to Fig. 5.3

	DISC <sub>1</sub>	DISC <sub>2</sub>	DISC <sub>3</sub>	DISC <sub>4</sub>
GENC <sub>1</sub>	C <sub>11</sub>	C <sub>12</sub>	C <sub>13</sub>	C <sub>14</sub>
GENC <sub>2</sub>	C <sub>211</sub>	C <sub>22</sub>	C <sub>23</sub>	C <sub>24</sub>
GENC <sub>3</sub>	C <sub>31</sub>	C <sub>32</sub>	C <sub>33</sub>	C <sub>34</sub>
GENC <sub>4</sub>	C <sub>41</sub>	C <sub>42</sub>	C <sub>43</sub>	C <sub>44</sub>

Each unit in Table: 5.1 symbolize a division of a total load contracted by a DISCO (column) towards a GENCO (row). Thus, the total power contracted by a DISCO j from GENCO i is corresponding to the ij-th entry. The summation of the entries in each column of the matrix is unity. DPM shows how the DISCO is in contract with a GENCO, and hence the “DISCO participation matrix”

In chapter-4, Block diagram of AGC of two area system under conventional scenario has been presented .In this chapter; the design of the block diagram for a two area AGC system in the restructured scenario is presented. With a change in the load demand by a DISCO, the local load in the area to which

this DISCO belong changes. This corresponds to the local loads DPL1 and DPL2 and should be reflected in the deregulated AGC system block diagram at the point of input to the power system block.

Since there are more than one GENCO in each area, ACE signal is distributed as per the participation in AGC among all the GENCOs. Coefficients that allocate ACE to numerous GENCOs are named as ACE participation factors. Fig.5.4 depicts the model of a two area system after restructuring.

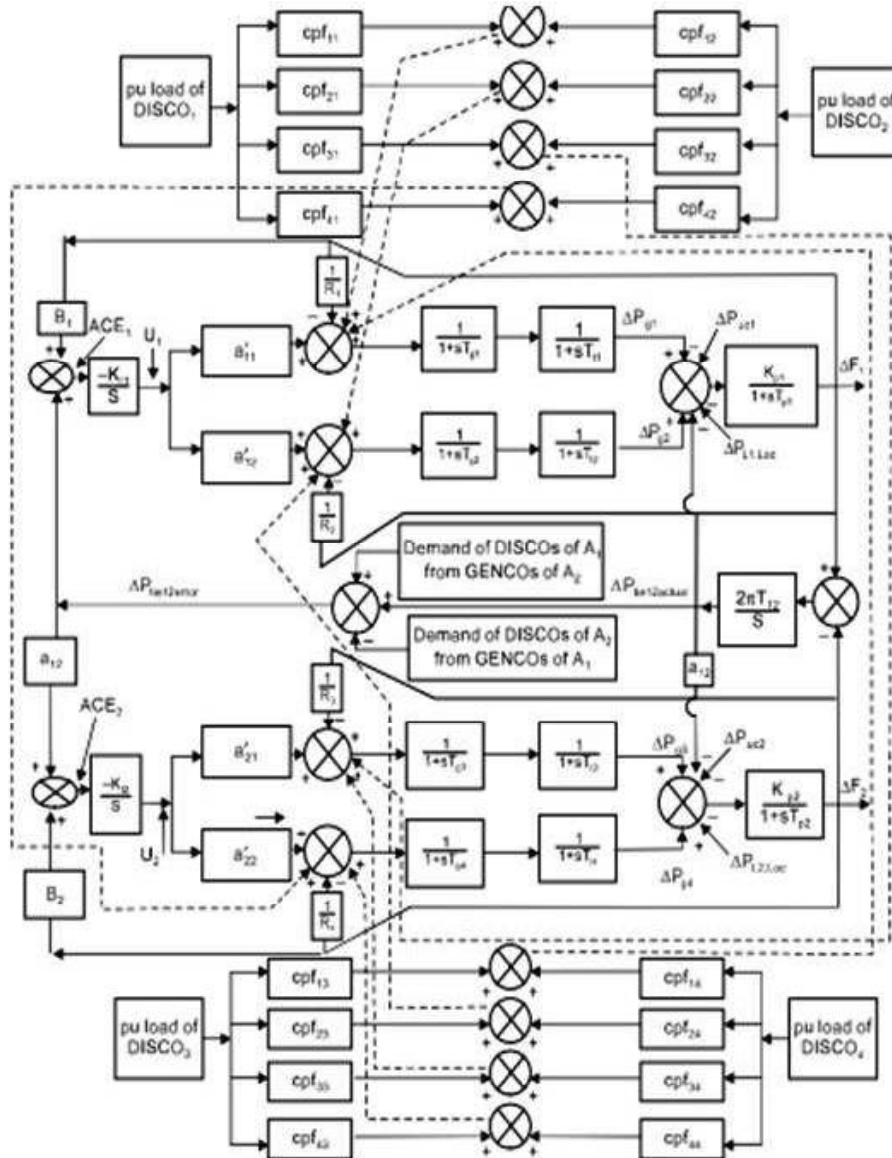


Figure 5.4 Block Diagram Representation of a two area system after Restructuring

#### 5.4 SIMULINK MODEL OF A TWO AREA AGC AFTER DEREGULATION

The SIMULINK model of a two area AGC [45] in the restructured power system is designed as shown in the Fig.5.5. A case is considered where there is an equal participation in AGC by GENCOs of each area. We assume that the load disturbances occur only in Area 1. Thus there is a load demand only by DISCO<sub>1</sub> and DISCO<sub>2</sub>. The load demand of 0.08 pu MW for each of the DISCOSs are considered, i.e,  $\Delta PL_1=0.08$  pu MW,  $\Delta PL_2=0.04$  pu MW,  $\Delta PL_3= \Delta PL_4=0$ . Now for this scenario the DPM is

$$DPM = \begin{pmatrix} \begin{array}{c|c|c|c} \mathbf{0.50} & \mathbf{0.50} & \mathbf{0} & \mathbf{0} \\ \hline \mathbf{0.50} & \mathbf{0.50} & \mathbf{0} & \mathbf{0} \\ \hline \mathbf{0} & \mathbf{0} & \mathbf{0} & \mathbf{0} \\ \hline \mathbf{0} & \mathbf{0} & \mathbf{0} & \mathbf{0} \end{array} \end{pmatrix}$$

The above DPM is implemented as a sub system in the MATLAB SIMULINK. The schematic of the DPM is shown in Fig. 5.5

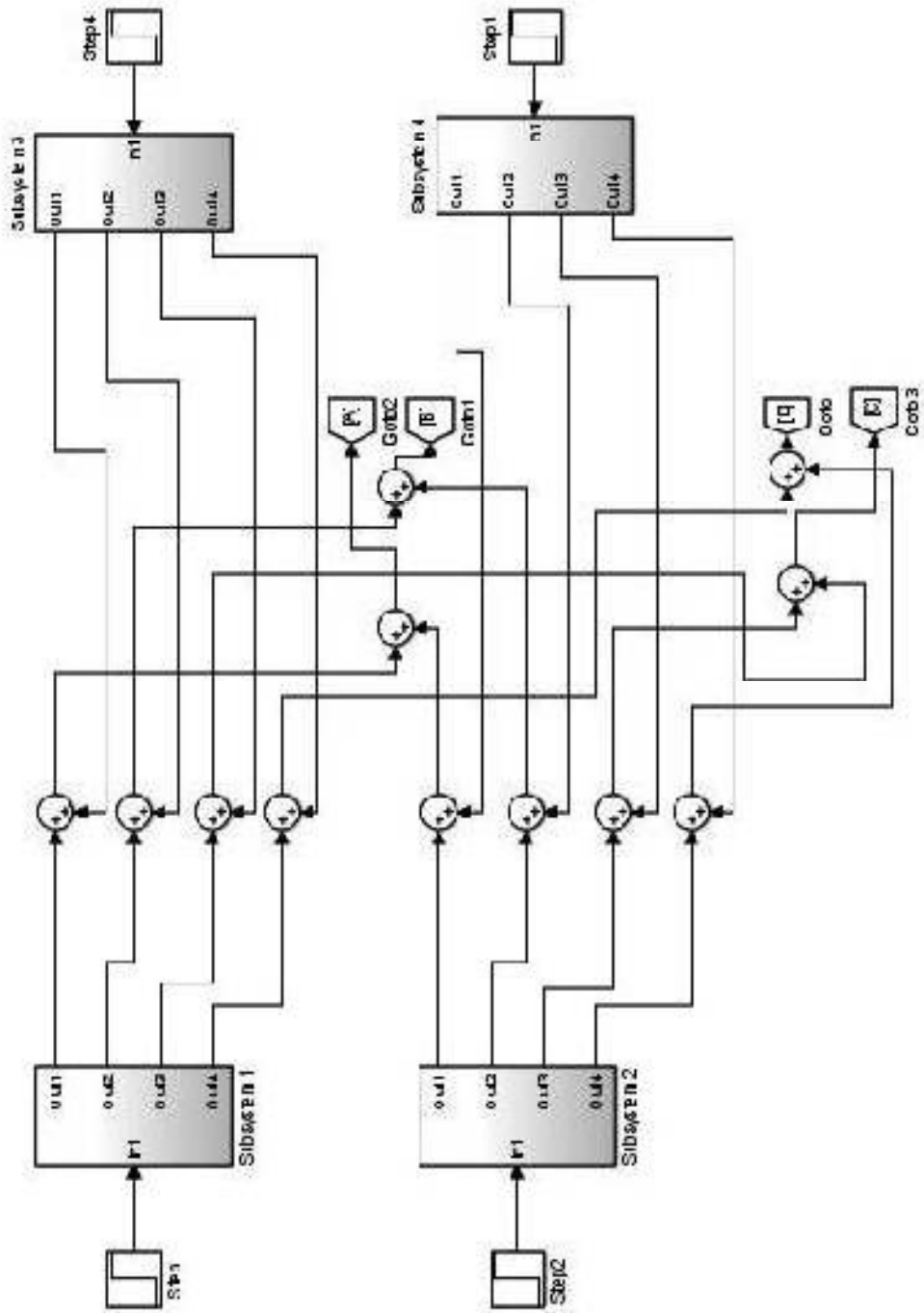


Figure 5.5 Simulink implementation of Disco participation





## 5.5 DESIGN OF CONTROLLER

The Simulink model shown in Fig. 5.6 is simulated with conventional PI controller. The results reveal that the time response specifications obtained is poor in terms of Overshoots, Undershoots and settling time. Hence there is a necessity of an intelligent controller which are robust, adaptive and can substantially lower the disturbances in terms of overshoots and undershoots and reduce the settling time [53]-[57]. However the response of the system with PI controller is captured for the purpose of comparison. The section 5.6 describes the construction of Fuzzy logic based controller using the expert knowledge of the system.

## 5.6 Design of Fuzzy Logic Controller

A Fuzzy logic controller is constructed with ACE and  $d/dt(ACE)$  as the two inputs using Fuzzy logic Tool box in MATLAB as shown in Fig. 5.7.

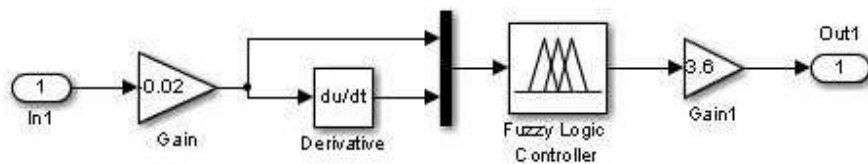


Figure 5.7 Fuzzy Logic Controller with gains

The two inputs (ACE and  $d/dt(ACE)$ ) and one output are described with five membership functions which are taken as symmetrical, extended over the universe of discourse as shown in Fig. 5.8

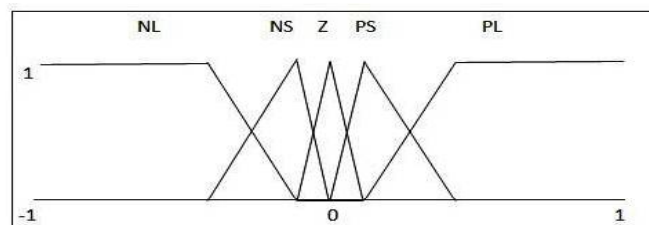


Figure 5.8 Structure of Membership function

A typical rule base as described in the Table 5.2 is used for the FLC. Initially, the FLC gains were chosen so as to allow the different variables (such as ACE,  $d/dt(ACE)$  and Output) hover within their respective Universes of Discourse (UODs).

**Table 5.2** Fuzzy Rule Base  
 $d/dt(ACE)$

	NL	NS	Z	PS	LP
NL	NL	NL	NS	NS	Z
NS	NL	NS	NS	Z	PS
Z	NS	NS	Z	PS	PS
PS	NS	Z	PS	PS	PL
PL	Z	PS	PS	PL	PL

The Gains of the FLC in each area are chosen so as to get the desirable response. Each FLC constitutes two gains, therefore for the model of the system in Fig. 5.6 have the gains K1, K2 for the FLC1 in the first area and the gains K3, K4 for the FLC2 in second area. In total there are four gains which are required to be chosen to deliver the desired performance.

Initially the FLC is constructed using symmetrical mfs with the gains K1, K2, K3 and K4 chosen by hit and trial. The response of the hand tuned FLC reveals that there is a scope of improvement in FLC by evolving the parameters of the gains of FLC using an intelligent optimization technique. However the response of Fuzzy controller without optimization is captured for the purpose of comparison. Section 5.7 describes the process of applying Genetic Algorithm technique to find the optimal values of the gains of FLC.

### 5.7 OPTIMAL TUNING OF THE GAINS OF FLC USING GA

With the knowledge gathered from various sources [58]-[64], GA is utilized to find the optimal gains of the fuzzy controller to improve its

performance. The structure of the chromosome is decided based on the sets of parameters of gains.

The initial population consists of thirty chromosomes. The structure of each chromosome is decided based on the sets of parameters of gains. There are two gains each in the FLC of Area-1 ( $K_1, K_2$ ) and Area-2 ( $K_3, K_4$ ), thus each chromosome contains  $[2+2]=4$  bits (genes). The method of roulette-wheel selection is used for selection of chromosomes for recombination. The crossover and mutation parameters are taken as 0.003 and 0.6 respectively.

The objective function, taken as Integral of Time multiplied Absolute Error (IATE) is minimized. The following equation Eqn. 5.1 represents the objective function:

$$J = ITAE = \int_0^{t_{sim}} (|\Delta F_1| + |\Delta F_2| + |\Delta P_{tie}|) \cdot t \cdot dt \quad \text{Eqn. (5.1)}$$

$\Delta F_1$  = Frequency deviation in Area-1.

$\Delta F_2$  = Frequency deviation in Area-2.

$\Delta P_{tie}$  = Tie Line Power deviation.

$t_{sim}$  = Simulation time.

The applied GA steps are summarized as follows:

1. The initial population of 30 random real coded strings of length 4 has been built (each controller gains by two genes).
2. The strings are represented by real numbers with values specified between the lower and upper bounds given in Table 5.3.

TABLE 5.3 BOUNDS FOR OPTIMAL GAINS

GAIN	LOWER BOUND	UPPER BOUND
K1	-0.005	-0.05
K2	1	4
K3	-0.005	-0.05
K4	0.5	4

### 5.7.1 RUNNING THE GA

GA was run for a number of generations, the detail of the Generation 1 statistics is listed in Table 5.4. The best controller was found during Generation 28. This run was continued further, and termination criterion was reached in generation 34. Few landmarks in generation statistics are shown in table 5.5.

Table 5.4 Population report for Generation 1

S.No	K1	K2	K3	K4	IATE
1	-0.0123	3.3829	-0.0432	3.7690	2.4890
<b>2</b>	<b>-0.0481</b>	<b>3.8947</b>	<b>-0.0121</b>	<b>2.7893</b>	<b>1.2251</b>
3	-0.0125	2.8059	-0.0168	2.7893	1.3997
4	-0.0125	2.8059	-0.0168	2.7893	1.6618
5	-0.0240	1.7533	-0.0327	2.1565	2.6786
6	-0.0138	3.7472	-0.0406	3.8582	1.4083
7	-0.0369	3.2641	-0.0174	2.8790	2.2575
<b>8</b>	<b>-0.0134</b>	<b>2.4693</b>	<b>-0.0251</b>	<b>2.7621</b>	<b>3.2637</b>
9	-0.0175	3.8779	-0.0296	0.9852	1.9112
10	-0.0451	1.1385	-0.0094	3.3821	2.2502
11	-0.0123	1.4878	-0.0104	2.2443	2.7293
12	-0.0345	3.3829	-0.0190	2.3499	1.3576
13	-0.0345	1.4878	-0.0104	2.2443	2.2595
14	-0.0481	2.4561	-0.0410	0.9966	1.6079
15	-0.0153	3.7400	-0.0119	3.3904	1.9988
16	-0.0175	1.1385	-0.0094	3.3821	1.2402
17	-0.0345	1.1071	-0.0432	3.7690	3.2140
18	-0.0345	1.5136	-0.0368	0.6114	1.9459

19	-0.0175	1.1385	-0.0368	0.6114	3.0698
20	-0.0345	1.5136	-0.0094	3.3821	1.8531
21	-0.0345	1.1071	-0.0432	3.7690	1.7779
22	-0.0175	1.1385	-0.0094	3.3821	2.0095
23	-0.0345	1.4878	-0.0104	2.2443	1.5530
24	-0.0345	1.1071	-0.0432	3.7690	1.8021
25	-0.0125	2.8059	-0.0168	3.8971	2.4457
26	-0.0481	3.8947	-0.0121	2.789	2.6534
27	-0.0416	1.7306	-0.0468	1.7249	1.3595
28	-0.0360	3.2445	-0.0253	0.7934	2.0700
29	-0.0117	1.7725	-0.0428	1.3900	1.3418
30	-0.0292	3.9884	-0.0085	2.0494	2.4941

It is evident from the Table 5.4 above that there is diversity in the fitness values of different chromosomes from the minimum fitness to the maximum fitness in the first generation. The aim is to produce a best fit chromosome in the generations to come.

The summary of the population report of generation 1 is as follows:

Maximum fitness function	=	1.2251			
Maximum fit chromosome	=	-0.0481	3.8947	-0.0121	2.7893
Minimum fitness Function	=	3.2637			
Minimum fit chromosome	=	-0.0134	2.4693	-0.0251	2.7621
Best fitness function	=	1.2251			
Best fit chromosome	=	0.0481	3.8947	-0.0121	2.7893

Table 5.5 A few landmarks in Generation Statistics.

Generation	Min Fit Function	Max Fit Function	Best fit Function	Best Fit Chromosome
1	3.2637	1.2251	1.2251	-0.0481 3.8947 -0.0121 2.7893
2	3.9543	1.1504	1.1504	-0.0446 3.4533 -0.0167 2.5802
3	3.9543	1.1504	1.1504	-0.0446 3.4533 -0.0167 2.5802
4	3.2367	1.0041	1.0041	-0.0481 3.8947 -0.0121 0.6206
9	2.8637	0.9931	0.9931	-0.0500 3.8779 -0.0296 0.9853
16	3.0034	0.9625	0.9625	-0.0482 3.9984 -0.0085 2.0494
24	3.0698	0.9691	0.9625	-0.0483 3.9884 -0.0088 2.5095
28	3.2637	0.9614	0.9614	-0.0481 3.8947 -0.0121 0.6207
34	3.4621	1.0013	0.9614	-0.0481 3.8947 -0.0121 0.6208

Table 5.5 compares the statistics of different generations. The termination criterion was reached in 34<sup>th</sup> generation. It is seen that the GA produced some good solutions (with fitness values 1.1504, 1.0041, 0.9931, 0.9625, 0.9614 in different generations), however, one of the solutions (i.e with fitness 0.9614) was the best fit in 34 generations.

### 5.8 SYSTEM SUBJECTED TO VARIOUS TESTING CONDITIONS

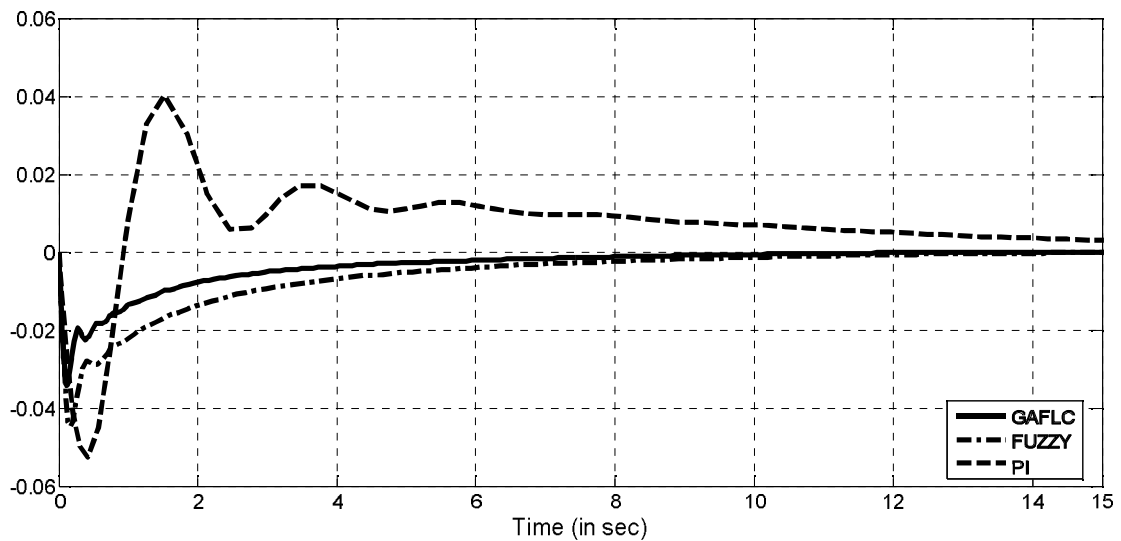
The Simulation is carried out on a two area deregulated interconnected system. Conventional PI controller and Fuzzy Logic Controller with and without Genetic Algorithm technique are implemented. Simulation is performed by applying a load variation of 0.08 pu in Area 1. The optimal parameters of the FLC gains as shown in Table 5.6 are obtained in 34 generation corresponding to the maximum fitness function.

Table 5.6 Optimized GAFLC parameters

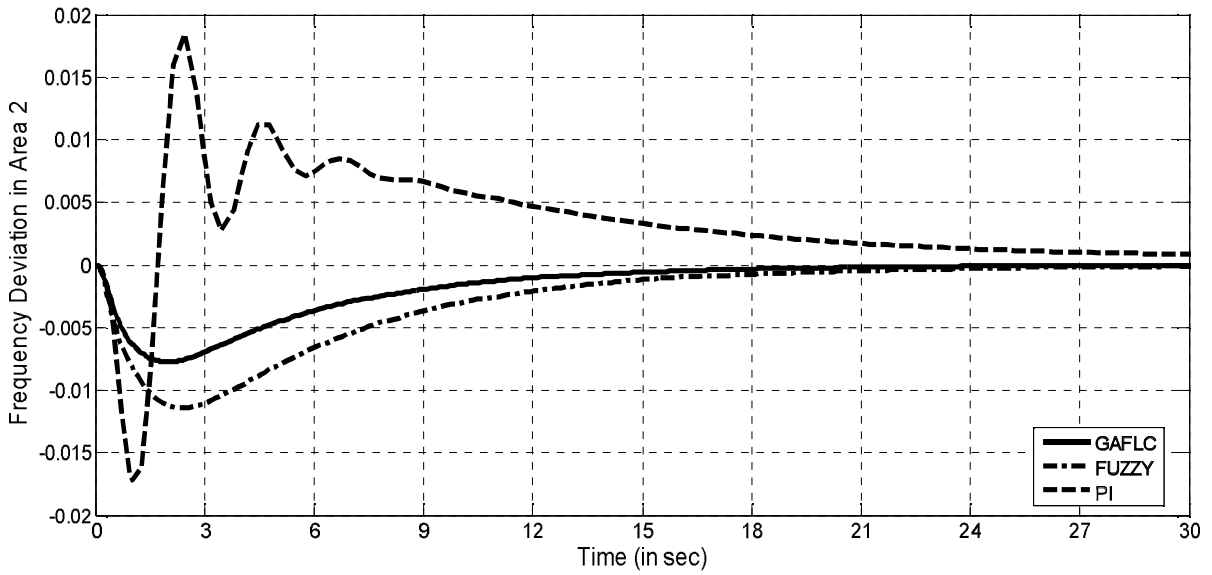
Controller	Objective Function Values	Optimal Controller Gains			
	(IATE)	K1	K2	K3	K4
GA FLC	0.9625	-0.0481	3.8947	-0.0121	0.6208
FLC HAND-TUNED	1.823	-0.02	3.6	-0.05	0.5

### 5.8.1 SYSTEM WITH NOMINAL PARAMETERS

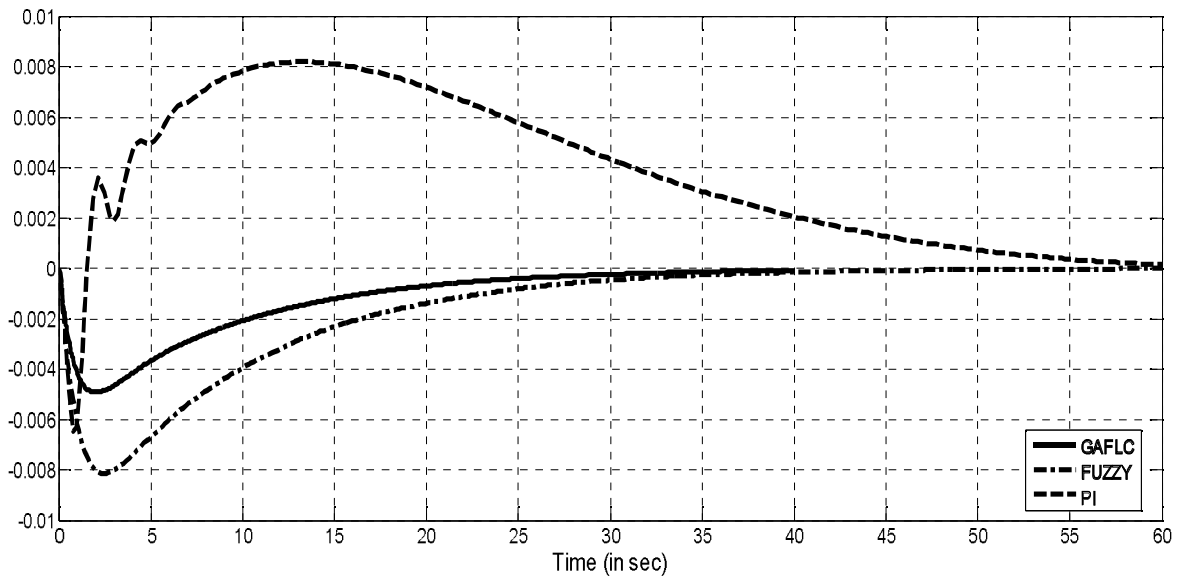
The dynamic response comparison between conventional PI, Hand tuned Fuzzy controller and GA tuned Fuzzy controller for frequency deviation in Area 1 ( $\Delta f_1$ ), frequency deviation in Area 2 ( $\Delta f_2$ ) and the tie-line power deviation ( $\Delta P_{tie}$ ) is portrayed in Fig. 5.9



a) Frequency Deviation (Area 1)



b) Frequency Deviation (Area 2)



c) Tie-Line power Deviation

Figure 5.9 Comparison of PI, Hand-tuned FLC & GA-tuned FLC response



It is noticeable from Fig. 5.9 that the overshoots, undershoots and settling time in  $\Delta f_1$ ,  $\Delta f_2$  and  $\Delta P_{tie}$  with the proposed GAFLC are significantly reduced as compared to PI and Hand tuned FLC. The transient response specifications of  $\Delta f_1$ ,  $\Delta f_2$  and  $\Delta P_{tie}$  in terms of  $U_{sh}$ ,  $O_{sh}$  and  $T_s$  (with 0.005% tolerance band) for PI, Fuzzy and GA Fuzzy controllers are illustrated in the Table 5.7. The statistics shows that system performance is remarkably enhanced by using intelligent GAFLC controller.

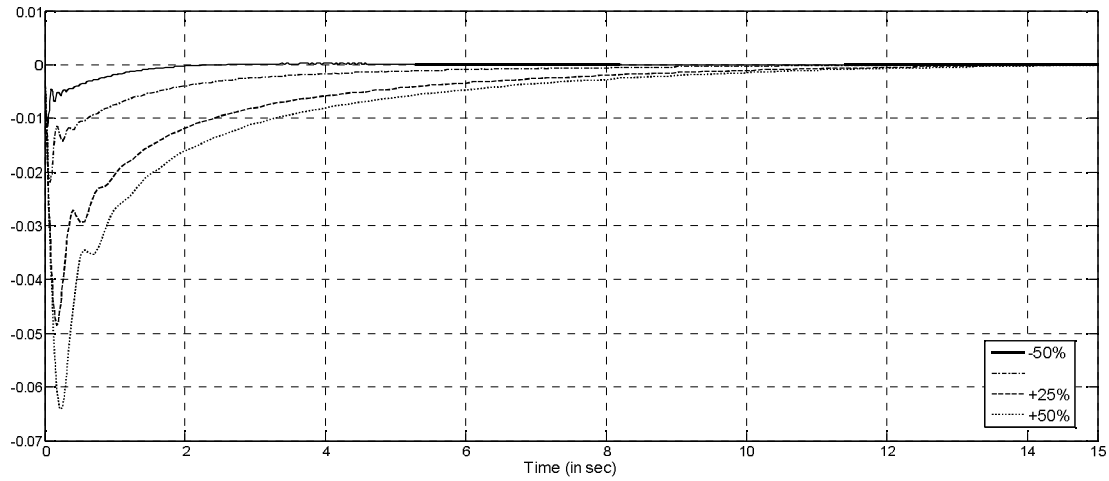
Table 5.7 Performance Comparison of GAFLC, Fuzzy and PI Controller

Controller	$\Delta f_1$			$\Delta f_2$			$\Delta P_{tie}$		
	$U_{sh}$ ( $\times 10^{-3}$ )	$O_{sh}$ ( $\times 10^{-5}$ )	$T_s$ (in sec)	$U_{sh}$ ( $\times 10^{-3}$ )	$O_{sh}$ ( $\times 10^{-3}$ )	$T_s$ (in sec)	$U_{sh}$ ( $\times 10^{-3}$ )	$O_{sh}$ ( $\times 10^{-3}$ )	$T_s$ (in sec)
GAFLC	-34.34	13.41	2.8	-7.731	0	4.5	-4.934	0	2.08
FUZZY (Hand tuned)	-44.94	17.25	5.03	-11.39	0	7.3	-8.139	0	7.6
PI	-52.73	4013	11.9	-17.1	18.43	11.29	-6.487	8.192	27.5

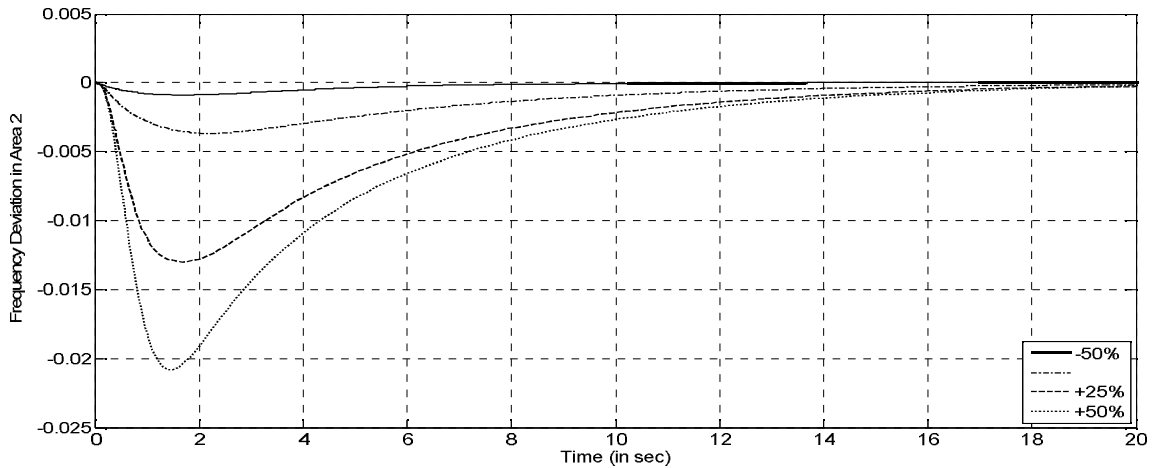
### 5.8.2 SYSTEM SUBJECTED TO PARAMETRIC DISTURBANCES

Sensitivity analysis is carried out on the original system by varying the parameters within allowable range [57], [58]. System parameters ( $T_g, T_r, T_t, T_p$ ) are varied in steps of 25% from -50% to +50% of their supposed values. Fig. 5.10

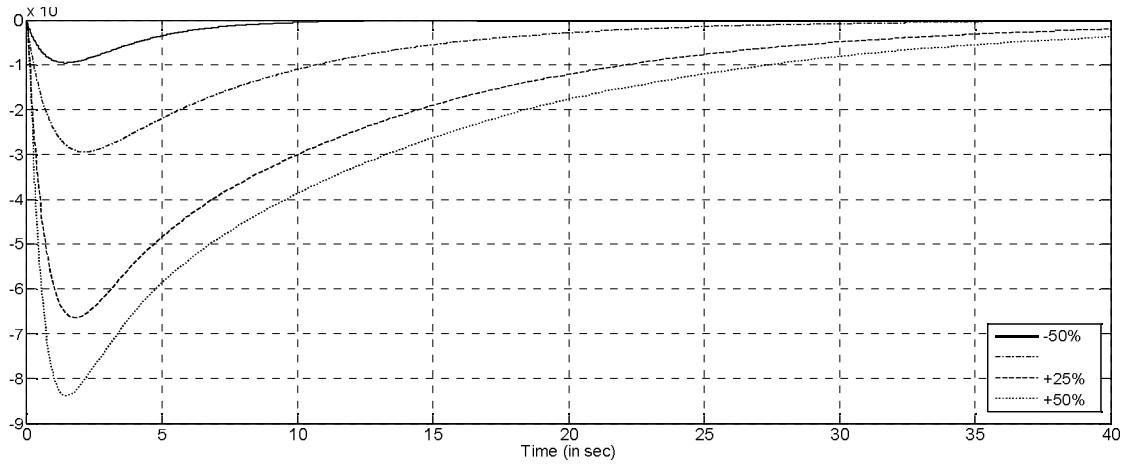
portrays the response of  $\Delta f_1$ ,  $\Delta f_2$  and  $\Delta P_{tie}$  under different parametric changes. Table 5.8 shows the performance indices under different parametric changes. It is observed that with the similar set of earlier optimized values of the gains, the GA-tuned FLC is able to seize the parametric disturbances well within the tolerable limits, thus tackling the problem of load frequency control.



a) Deviation in Frequency (area 1)



b) Deviation in Frequency (area 2)



c) Deviation in Tie Line power

Figure 5.10 Response comparison with system subjected to parametric variations

Table 5.8 Sensitivity analysis with parametric variations

System Parameters	% Change	$\Delta f1$			$\Delta f2$			$\Delta P_{tie}$		
		Ush ( $\times 10^{-3}$ )	Osh ( $\times 10^{-5}$ )	Ts	Ush ( $\times 10^{-3}$ )	Osh ( $\times 10^{-5}$ )	Ts	Ush ( $\times 10^{-3}$ )	Osh ( $\times 10^{-5}$ )	Ts
Tg, Tr, Tt, T <sub>P</sub>	-50%	-11.54	22.76	0.93	-0.88	0	0	-0.953	0	0
	-25%	-21.84	3.8	3.51	-3.65	0	0	-2.93	0	0
	+25%	-48.51	24.57	5.2	-12.97	0.12	0.42	-6.64	0	6.6
	+50%	-64.2	36.88	6.53	-20.78	3.29	0.37	-8.38	0	9.56

### 5.8.3 SYSTEM WITH DYNAMICALLY CHANGING GENERATOR MODEL

The controller is tested on dynamic model of AGC with parameters of generator varying with time. The transfer function of the generator model may vary with time with changes in the parameters of the transfer function. The general transfer function of the generator model is given by  $K_p / T_p s + 1$ . Fig. 5.11 shows the arrangement for changing the parameters of the transfer function while the simulation is in progress.

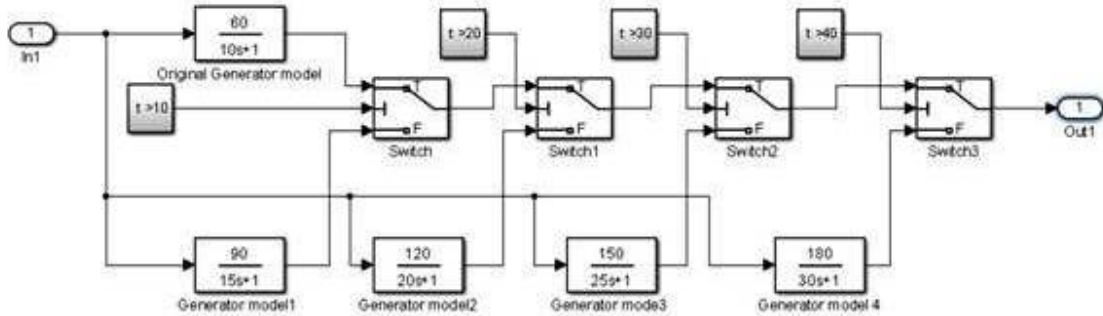


Figure 5.11 Switching Model for Parametric variation in Generator model

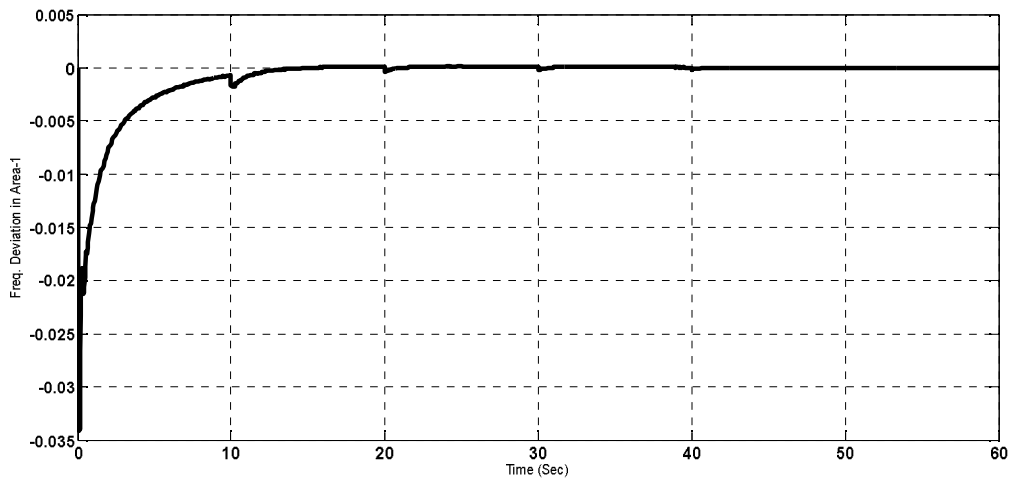
The system is tested with the parameters ( $K_p$  and  $T_p$ ) varying in the range from -50% to + 50 % of their nominal values as per Table 5.9

Table 5.9 Variations in Generator model transfer function

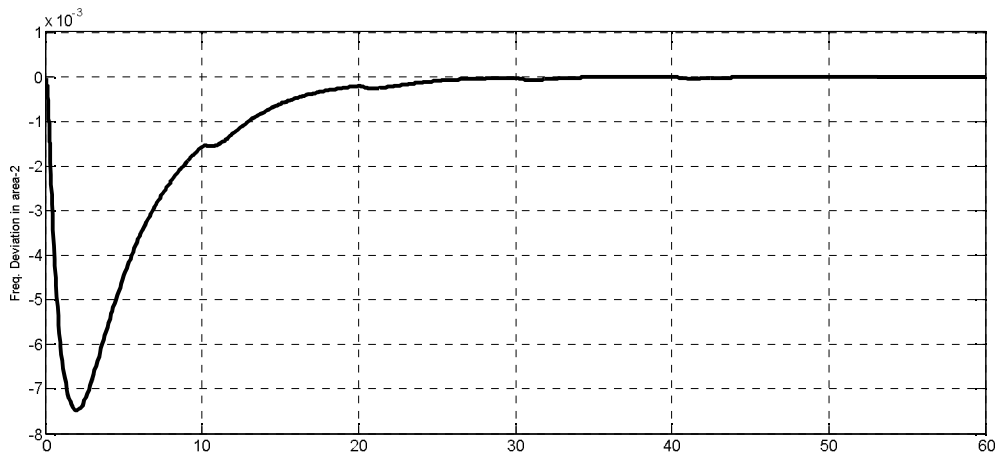
% Change	$K_p$	$T_p$
-50%	60	10
-25%	90	15
Nominal	120	20
+25%	150	25

+50%	180	30
------	-----	----

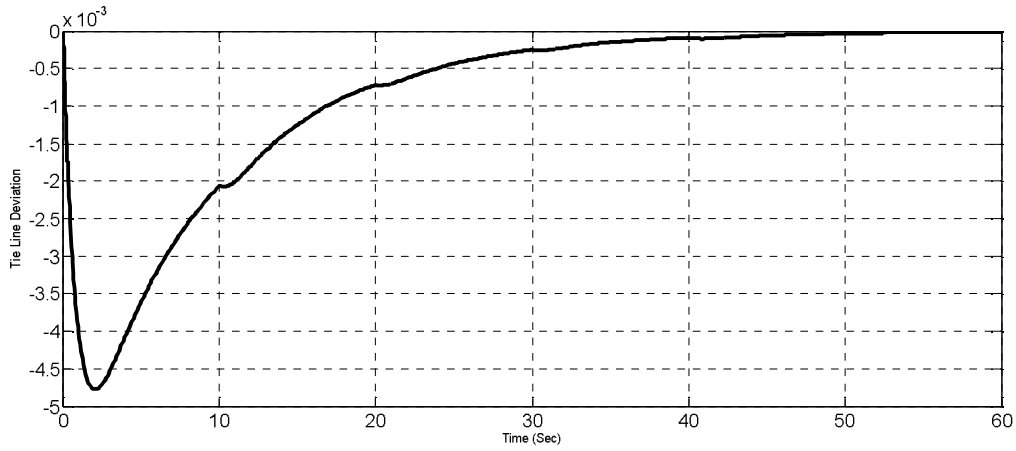
The switching system shown in Fig. 5.11 is incorporated in Area -1 of the two Area AGC model under restructured scenario and the response of the system is captured with parameters of the transfer function changing after 10 seconds in the range depicted in Table 5.9. The Figure 5.12 depicts the behavior of the dynamic system with changing transfer function model of the generator in Area-1.



a) Area-1 Response



b) Area-2 Response



c) Tie Line Deviation

Figure 5.12 Responses with varying Parameters of Generator model in area-1

Figure 5.12 depicts the performance of proposed intelligent controller (GA-tuned FLC) under the dynamically changing parameters of the generator model in Area 1. It is observed that the controller performance is robust and the response remain well within the tolerable range even under changing transfer function of generator every 10 seconds.

#### 5.8.4 SYSTEM WITH RANDOM LOAD DISTURBANCE PATTERN

To examine the efficacy of the proposed controller, random step load disturbances are injected to Area-1. after 10 seconds of operation. Fig. 5.13 shows the random step load disturbance pattern which is random both with respect to magnitude and time period [31]. The frequency deviation of Area-1 is illustrated in Fig. 5.14.

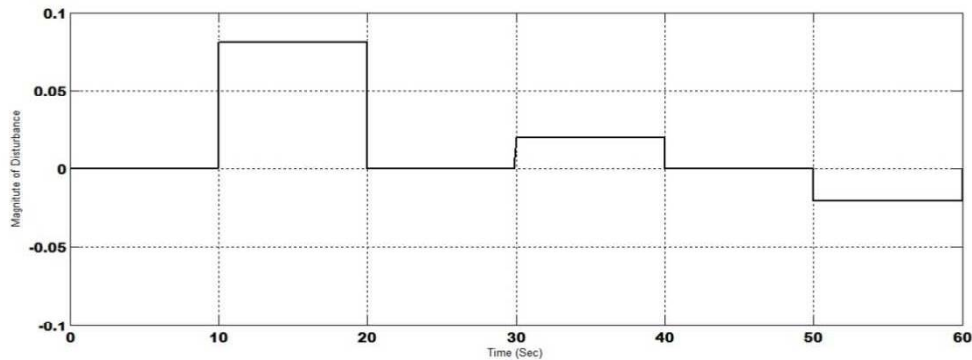


Figure 5.13 Pattern of Random step load disturbance

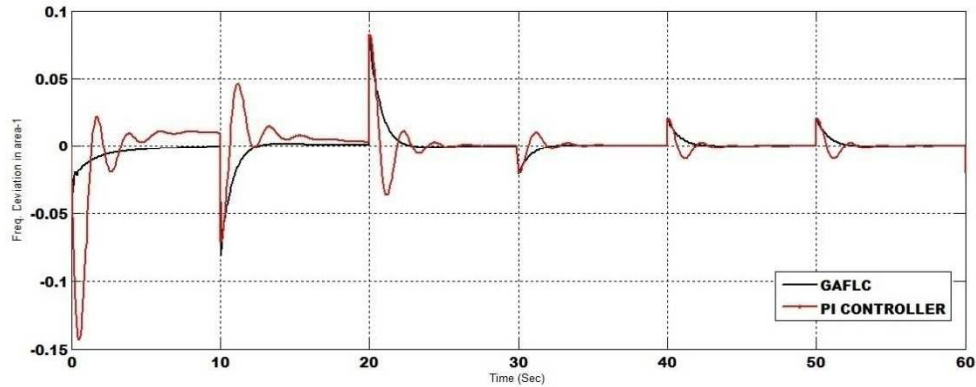


Figure 5.14 Frequency response under Random step load disturbance in area-1  
 It is apparent from the Fig. 5.14 that proposed intelligent controller delivers a better transient response under such random load disturbances as compared to the conventional PI controller.

## 5.9 CONCLUSION

In this chapter, FLC with and without GA is implemented for an Automatic Generation Control (AGC) of interconnected power system under Deregulation. Simulation results are compared with a conventional PI controller. As revealed in the simulation results, using the proposed method, the deviation in the tie-line power and frequency deviation of both the areas are driven near to zero. Furthermore, the proposed method of optimization using GA is very effective, i.e., it is able to find the local optimum solution to determine the system objective (minimizing control error), the intelligent controller offers smooth response, and deviation in frequency are a reduced in the same system with conventional controllers. Sensitivity analysis performed by varying the nominal parameters of the system over a wide range depicts the robustness of the proposed controller. Furthermore system is subjected to dynamically changing parameters of generator in Area-1 and random step load patterns are injected in Area-1 to test the robustness of the proposed intelligent controller. It is clear from the result that the proposed controller is very effective.